The Trade Wind Field Over the Pacific Ocean[1]

KLAUS WYRTKI AND GARY MEYERS

Department of Oceanography, University of Hawaii, Honolulu 96822

(Manuscript received 15 August 1975, in revised form 3 May 1976)

ABSTRACT

The trade wind field over the Pacific Ocean between 30°N and 30°S has been studied on the basis of five million wind observations made from ships. Data were sorted by quadrangles of 2° latitude and 10° longitude to resolve north-south gradients in the wind field adequately. Maps of the surface wind stress vector for February and August are presented and the development of the field throughout the year is discussed. The trade wind regime in each hemisphere is largest and strongest during the respective winter and spring. The area covered by northeast trades is smaller than the area covered by southeast trades, but the northeast trades have a stronger mean wind stress and a larger annual variation both in area and mean stress.

The computed divergence of the wind velocity revealed a little known area of convergence in the southeastern Pacific near the equator. The curl of the wind stress and the meridional profile of zonal wind stress vary considerably during the year. The minimum in zonal stress between the northeast and the southeast trades is a poorly developed feature from January to March while the maximum northeast trades are south of their mean position. Averaging the zonal stress over the South Pacific is deceptive because of large zonal variations.

Time series of the Pacific Ocean area covered by northeast and southeast trades, the mean zonal wind stress within the area, and the mean zonal wind stress in large, fixed areas are presented for the period from 1947 to 1972. The southeast trades covered an anomalously large area during 1955–56, 1964, 1966–67 and 1970–71. Interannual variations of the northeast trades are smaller than those of the southeast trades. There is no apparent relationship between fluctuations in the strength and areal extent of the northeast and southeast trades, except with the annual cycle.

1. Introduction

The trade wind field over the Pacific Ocean is one of the largest and most consistent wind fields on our globe. Although its general characteristics and annual variations are well established, little is known about its fluctuations in time and space. Details of the field such as the location of its boundaries and the shape of the meridional wind profile are lacking. This is largely due to the fact that 5° squares are used in averaging data in climatological studies, while a north-south grid space of about 2° is required. The large-scale features of the field and its annual variations were first studied by Crowe (1951a, b), who recognized the need to use direct wind observations in the tropics. More recently, Hellerman (1967) computed mean seasonal wind stress values in 5° squares. His basic data for the Pacific were wind roses taken from atlases published before 1960. The number of wind observations has increased considerably since the atlases were compiled and it is now possible to study the large-scale, interannual variations during the period after World War II. The field of wind stress and its fluctuations are of particular interest to physical oceanographers in their studies of the wind-driven ocean circulation since the curl of the wind stress is a parameter in their computations.

We have used nearly five million wind observations of ships taken from the marine deck of the Environmental Data Service, Asheville, N. C., to study the annual and interannual variations of the Pacific trade wind field. The original data, data processing, and all the derived data are described in a technical report (Wyrtki and Meyers, 1975a, b). In processing the data the original Beaufort estimates were converted to wind speeds using the World Meteorological Organization's Code 1100. [Use of the Beaufort scale for scientific purposes has been discussed by Kinsman (1968) and Dury (1970).] The observations were sorted in quadrangles of 2° latitude by 10° longitude, and the velocity and wind stress were averaged for various periods: individual months, individual bimonthly periods, long-term monthly means, and the long-term annual mean. All the observations in the deck taken prior to 1973 were used to compute the long-term means. Averages for individual months were computed only for the period after 1947.

The wind stress has the same direction as the wind velocity and its magnitude is given by

$$\tau = \rho_a C_D W^2, \qquad (1)$$

where τ is the wind stress, ρ_a the density of the air, C_D the drag coefficient and W the wind speed. The stress was computed from each wind observation before

[1] Hawaii Institute of Geophysics Contribution No. 769.

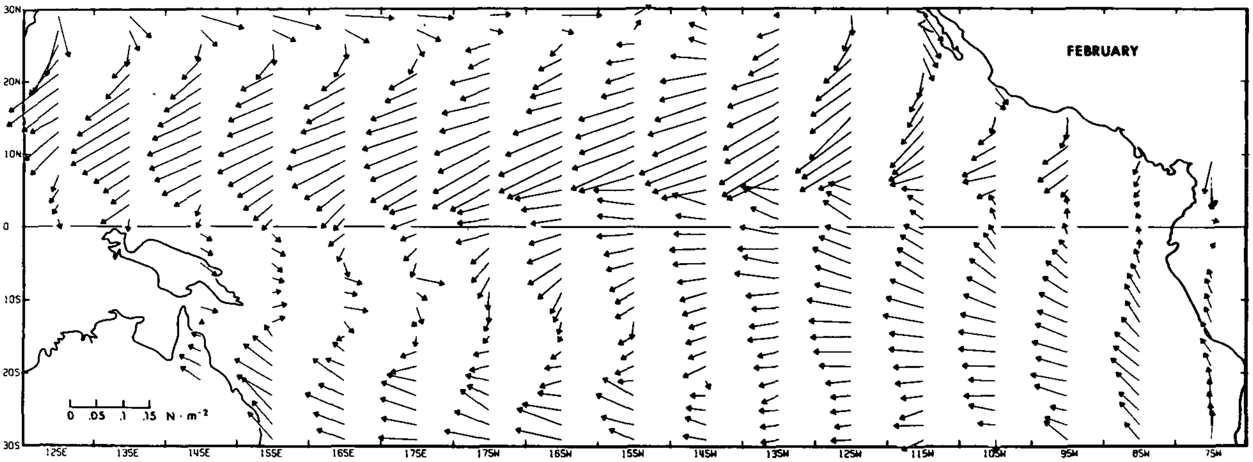

FIG. 1. Surface wind stress for February.

averaging. Constant values were used for ρ_a (1.2 kg m^{-3}) and C_D (1.5×10^{-3}). Our wind stress values are in excellent agreement with Hellerman's concerning the stress magnitude (Wyrtki and Meyers, 1975a), but indicate a shift in the northeast trade wind direction toward a more zonal orientation. It is known that the northeast trade wind direction varies over long periods (Wentworth, 1949) and the difference in direction is probably due to the different time spans covered by the data.

2. Mean annual variations

Monthly maps of the wind velocity and wind stress vectors were published in the technical report. The wind stress maps for February and August are presented in Figs. 1 and 2. The area covered by trades was determined by summing the quadrangles in which the wind direction falls between northeast and southeast and the zonal component of the mean wind stress is greater than 0.036 N m^{-2}, corresponding to a mean wind speed of about 3 m s^{-1}. In the region between the equator and 10°N, northeast and southeast trades were differentiated according to the direction of the meridional component. This procedure yields areas which vary throughout the year (Fig. 3, top) in nearly the same way as the areas determined by Crowe (1951a), who defined the trade wind areas in terms of wind constancy. The mean zonal wind stress in each trade wind area also varies throughout the year (Fig. 3, bottom). The northeast trades are strong during the northern winter and spring and extend across the Pacific to Asia where they merge with the northeast monsoon (Fig. 1). In contrast, the southeast trades are weak at this time. Westerlies near New Guinea and a zone of weak convergent winds near the date line separate the southeast trades east of Australia from the main part of the trade wind belt in the eastern Pacific. Cloud cover measurements (Sadler, 1969) and computation of the divergence of wind velocity (Wyrtki

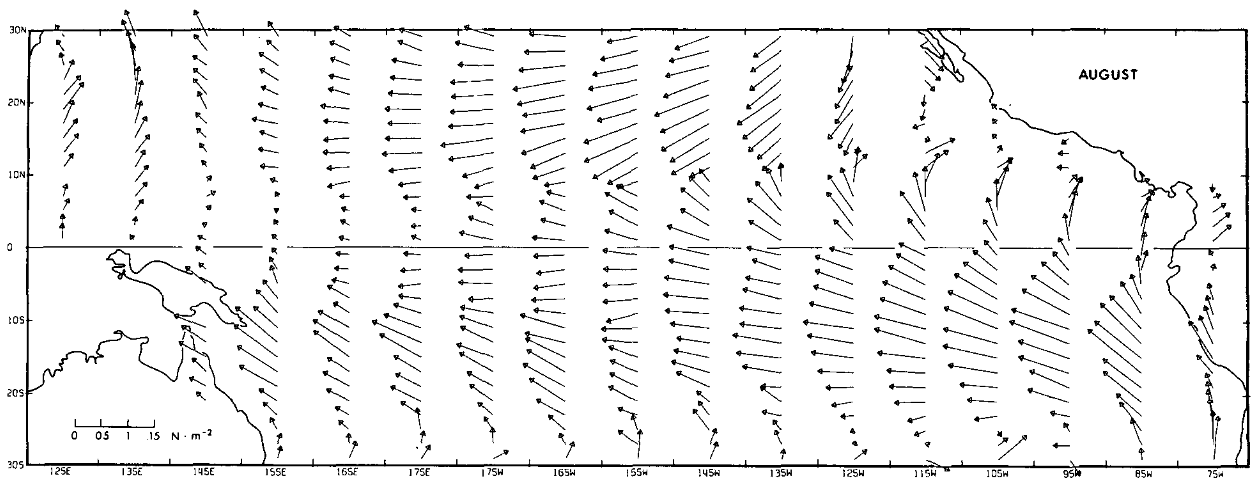

FIG. 2. As in Fig. 1 except for August.

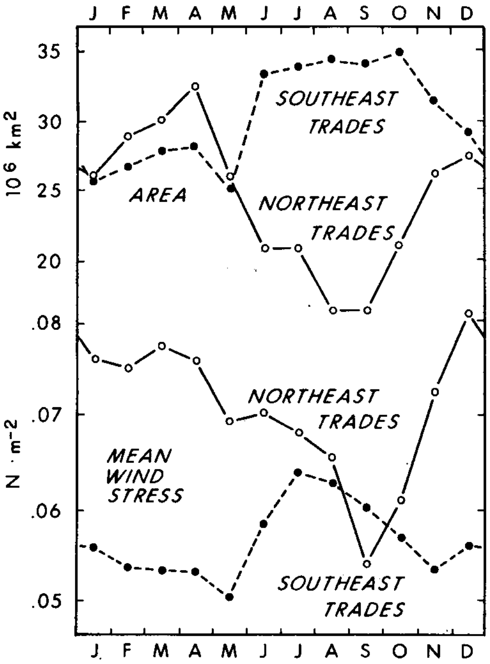

FIG. 3. Monthly variation of Pacific Ocean area covered by trades (top) and mean zonal wind stress within the area (bottom).

and Meyers, 1975a) indicate that the winds are convergent in this zone throughout the year. During the southern winter and spring the southeast trades are strong and extend across the Pacific to Australia (Fig. 2). Westerlies develop in the eastern Pacific near 10°N during this season. The northeast trades are weak and do not extend west of 150°E. Averaged over the year the area covered by northeast trades is smaller than the area covered by southeast trades, but the northeast trades have a stronger mean wind stress and a larger annual variation both in area and mean stress (Fig. 3).

The north-south grid space of 2° is particularly suitable for computing the wind divergence and wind stress curl, which depend largely on meridional derivatives. Annual and bimonthly maps of these derived fields were published in the technical report; the maps for March–April are shown in Figs. 4 and 5. Several features of the wind divergence correspond to well-known maxima and minima of cloud cover (Sadler, 1969), in particular, to the location of the Intertropical Convergence Zone between 5°N and 10°N in the central Pacific and a zone of convergence southeast of New Guinea. A little-known feature is the near-equatorial convergence south of the equator in the eastern Pacific, which appears throughout the year except November–December. It is most intense in March–April when the ITCZ is at its southernmost position; during that period it appears as a maximum in maps of the cloud cover (Sadler, 1969; Taylor, 1973).

The meridional profile of zonal wind stress and the curl of the wind stress are particularly relevant in theories of ocean circulation (Sverdrup, 1947; Munk, 1950). The zonal wind stress averaged across the Pacific varies considerably during the year (Fig. 6). The values at each latitude and the longitudinal limits for the zonal averages are given in Table 1. The northeast trade wind maximum is near 12°N from January to March, and the minimum between the northeast and the southeast trades is poorly developed. At that time, a band of intense positive curl is located between 10°N and the equator. The zonally averaged profile is nearly flat over the South Pacific during this season, indicating small values of the curl. However, this is a misleading result because in February and in the eastern Pacific the southeast trade wind maximum is located near 13°S, while in the western Pacific westerlies or calms occur at the same latitude. The field of wind stress curl (Fig. 5) shows two zones of negative curl over the eastern and western South Pacific divided by a zone of positive curl. This structure in the field prevails from November to April and appears in the annual mean field. From June to October distinct trade wind maxima occur in both hemispheres and are separated by a well-developed minimum between 6°N and

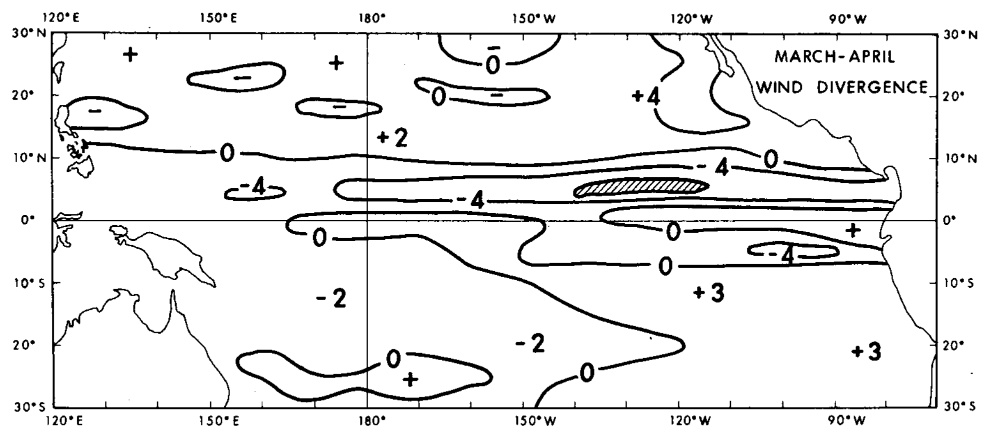

FIG. 4. Divergence of the wind velocity (10^{-6} s^{-1}) for March–April. Cross-hatching indicates convergence greater than -8×10^{-6} s^{-1}.

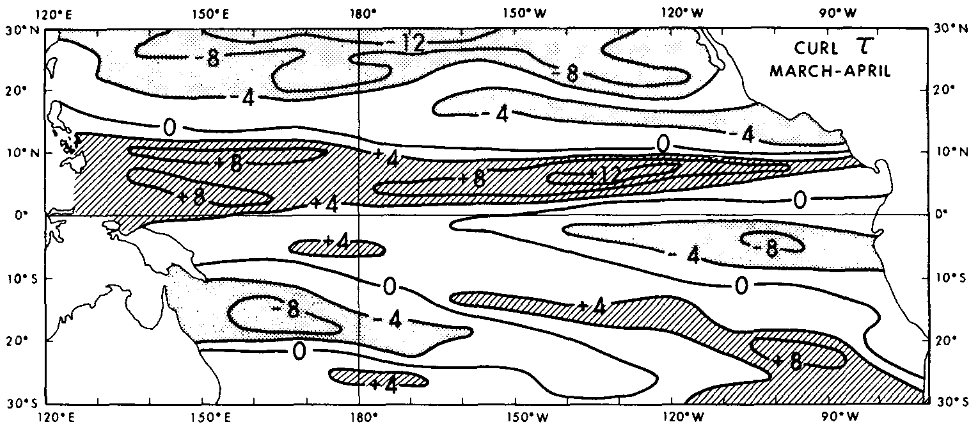

FIG. 5. Curl of the wind stress (10^{-8} N m^{-3}) for March–April.

10°N (Fig. 6). Meridional shifting of the wind minimum and of the northeast trade wind maximum results in a large change in wind stress curl in the region between the equator and about 15°N. Annual variation of the curl at 10°N has been related to changes in the North Equatorial Current by Meyers (1975). Another interesting feature of the southeast trade wind profile which is lost in the zonal average is seen on the stress map for August. In the region east of 130°W, a secondary maximum of zonal stress occurs north of the equator, resulting in a double band of negative curl in the southeast trades.

3. Interannual variations

Large year-to-year changes in the trade wind field are seen on bimonthly maps of the wind stress vector, particularly in the Southern Hemisphere (Wyrtki and Meyers, 1975b). The area and mean wind stress, as previously defined, were computed from monthly fields of wind stress (Fig. 7, top and bottom). The zonal component of stress (Fig. 7, center) was also averaged over large, fixed areas in the middle of the northeast and southeast trades (12°N to 24°N, 130°W to 150°E; 2°S to 16°S, 90°W to 160°W). Climatological

TABLE 1. Zonal wind stress over the Pacific averaged over the longitude range given in the last column. Units are 10^{-3} N m^{-2}.

	Month													
Latitude	Jan.	Feb.	Mar.	Apr.	May	June	July	Aug.	Sep.	Oct.	Nov.	Dec.	Annual	Longitude range
29°N	44	41	10	−22	−15	−5	−29	−30	−23	−29	−18	18	−4	130°E to 110°W
27°N	16	13	−12	−38	−26	−18	−43	−37	−31	−42	−35	−7	−21	130°E to 110°W
25°N	−2	−12	−30	−47	−35	−30	−51	−42	−38	−49	−47	−32	−35	130°E to 110°W
23°N	−22	−31	−44	−57	−44	−39	−53	−46	−42	−53	−60	−53	−45	130°E to 110°W
21°N	−46	−51	−59	−67	−53	−47	−56	−49	−45	−60	−72	−70	−56	130°E to 110°W
19°N	−61	−62	−70	−73	−60	−53	−56	−47	−44	−60	−81	−83	−63	130°E to 110°W
17°N	−71	−76	−79	−80	−64	−59	−56	−49	−38	−58	−84	−96	−67	130°E to 110°W
15°N	−84	−85	−87	−87	−73	−65	−54	−43	−33	−46	−86	−101	−70	130°E to 110°W
13°N	−92	−94	−93	−86	−76	−67	−48	−32	−22	−37	−77	−97	−68	130°E to 110°W
11°N	−91	−95	−95	−85	−75	−57	−33	−20	−14	−25	−61	−87	−61	130°E to 110°W
9°N	−88	−89	−84	−79	−61	−43	−26	−11	−5	−10	−44	−79	−51	130°E to 110°W
7°N	−69	−76	−69	−66	−44	−32	−22	−17	−10	−10	−30	−54	−42	140°E to 100°W
5°N	−54	−54	−55	−46	−35	−28	−24	−25	−18	−17	−29	−43	−36	140°E to 100°W
3°N	−43	−41	−36	−31	−31	−28	−35	−31	−26	−26	−28	−35	−33	140°E to 110°W
1°N	−34	−34	−28	−27	−29	−29	−36	−36	−31	−28	−30	−32	−31	140°E to 100°W
1°S	−36	−34	−26	−24	−33	−36	−42	−39	−37	−30	−32	−35	−34	150°E to 90°W
3°S	−40	−32	−31	−29	−33	−44	−50	−44	−43	−36	−38	−39	−38	150°E to 90°W
5°S	−33	−33	−31	−39	−35	−45	−54	−52	−48	−41	−37	−38	−40	150°E to 90°W
7°S	−32	−26	−32	−40	−38	−51	−59	−57	−55	−44	−39	−33	−42	150°E to 90°W
9°S	−28	−25	−33	−41	−42	−56	−65	−63	−57	−47	−37	−32	−44	150°E to 90°W
11°S	−33	−28	−37	−46	−47	−62	−70	−74	−65	−55	−42	−39	−50	160°E to 80°W
13°S	−35	−29	−36	−47	−48	−69	−76	−77	−70	−60	−44	−38	−52	160°E to 80°W
15°S	−39	−33	−37	−50	−48	−66	−70	−74	−65	−67	−49	−40	−53	160°E to 80°W
17°S	−39	−36	−37	−42	−44	−60	−62	−66	−63	−61	−50	−47	−50	160°E to 80°W
19°S	−36	−40	−40	−47	−40	−61	−55	−54	−60	−63	−53	−49	−50	160°E to 80°W
21°S	−38	−38	−46	−45	−33	−47	−43	−47	−54	−58	−47	−45	−45	160°E to 80°W
23°S	−40	−40	−43	−38	−23	−33	−27	−30	−41	−44	−43	−43	−37	160°E to 80°W
35°S	−36	−45	−49	−34	−17	−20	−10	−13	−30	−39	−34	−39	−30	160°E to 80°W
27°S	−34	−44	−42	−36	−7	−7	2	−4	−19	−30	−25	−27	−23	160°E to 80°W
29°S	−29	−42	−38	−22	2	20	13	17	−14	−20	−25	−23	−13	160°E to 80°W

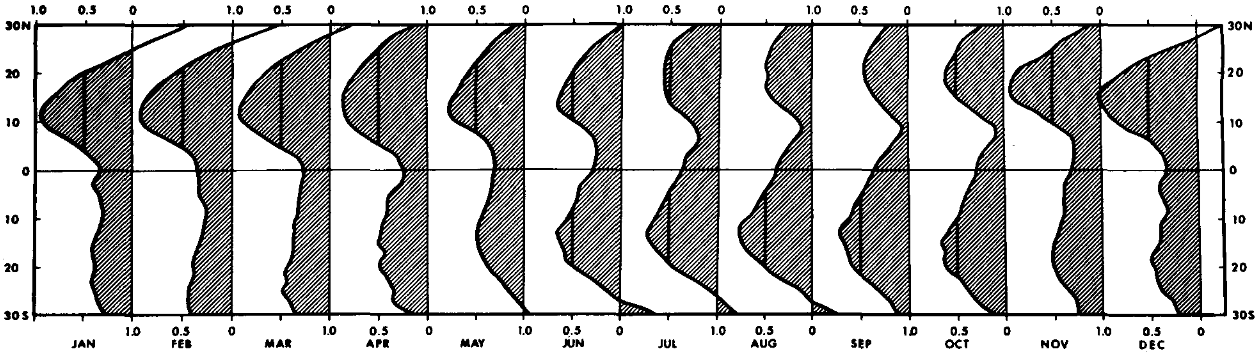

FIG. 6. Zonal wind stress over the Pacific Ocean averaged between the longitudes given in Table 1. 1 unit=0.1 N m⁻².

values were substituted for missing data in the monthly fields. The monthly values were low-pass filtered with 5-month and 12-month running means to reduce high-frequency fluctuations. Comparison of the two wind stress indices with the bimonthly maps showed that the zonal component (Fig. 7, center) is the better stress indicator for the southeast trades because it covers the main part of the wind belt in the eastern Pacific, while the mean wind stress (Fig. 7, top) is the better indicator for the northeast trades because it always covers the

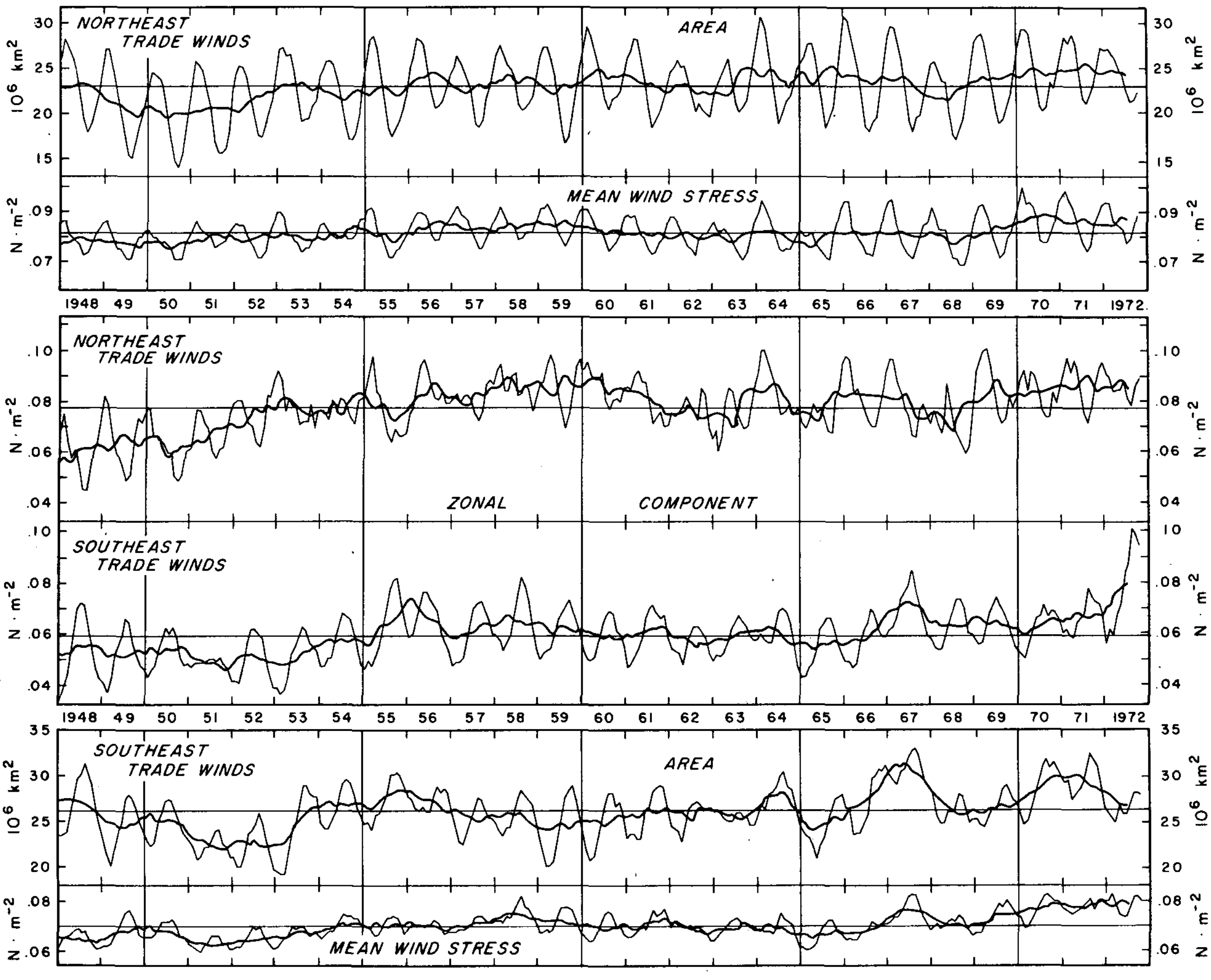

FIG. 7. Annual variation of area covered by northeast trades and mean zonal wind stress within the area (top); zonal wind stress averaged over 12°N–24°N, 130°W–150°E and 2°S–16°S, 90°W–160°W (center); and area covered by southeast trades and mean zonal wind stress within the area (bottom).

northeast trade wind maximum, which at times shifts south of 12°N.

Very large changes in the seasonal peaks of area and stress occur in the southeast trades. The area was largest during 1955–56, 1966–67 and 1970–71. The winds did not weaken as much as usual during the southern summers between these years. The area was also moderately large in 1964. The wind stress is generally strong when the area is large, except in 1972. The area covered by southeast trades was exceptionally small in 1951–52 and in 1965. The fluctuations in area are related to the onset of El Niño in 1957, 1965 and 1972 (Wyrtki, 1975). The area covered by northeast trades varies relatively uniformly each year. The annual variation in mean wind stress was severely interrupted only during 1954. The winter peak in wind stress was low in 1963 and 1965 and high in 1964 and 1966; however, this 2-year oscillation does not appear in the remainder of the time series. Both the northeast and the southeast trades were considerably weaker during the late 1940's and early 1950's than they were during the remainder of the period studied.

Variation in trade wind direction was investigated using the direction of the resultant wind stress vector in the two large fixed areas defined above. The trades in each area blow more directly toward the equator as the wind strengthens. This relationship appears in the 5-month and 12-month running means of direction and stress magnitude (not presented) but not distinctly in the monthly values. The mean annual range of direction is only 11° in the northeast trades and 13° in the southeast trades and the monthly standard deviations range from 3° to 8°. Although small, the variations in direction warrant further investigation since they lead to a large change in the length of trade wind trajectories from the eastern subtropical Pacific to the near-equatorial zones of convergence. A smaller length implies that the air is in contact with the sea surface for a shorter time and gains less moisture before reaching the zones of convergence, where the atmospheric circulation gains its energy through the release of latent heat. Thus, strong trades blowing more directly toward the equator tend to limit their own supply of latent heat. It is worth noting that fluctuations of the zonal component of wind stress (Fig. 7, center) and the magnitude of the wind stress are highly correlated (0.99) in each trade wind system due to the small variability in trade wind direction.

The curves in Fig. 7 suggest that large-scale anomalies of the tropical circulation occur over periods of more than one year. The wind fields derived from ships' observations during 1971 and 1972 (Wyrtki and Meyers, 1975b) were compared to the circulation at 700 mb derived from cloud motions by Krueger and Winston (1975). It was encouraging that the same anomalous features appeared in the independent data sets.

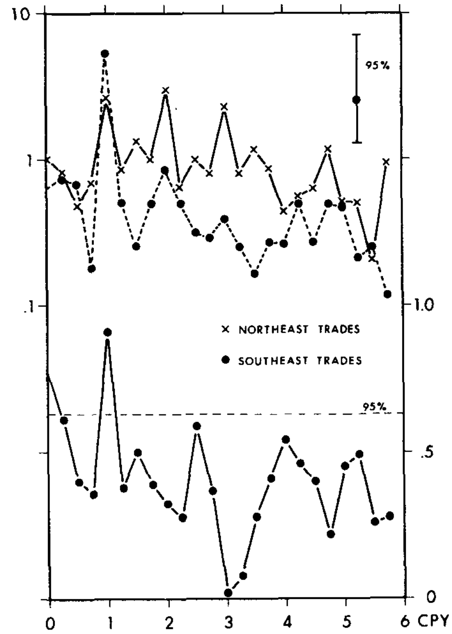

FIG. 8. Power (top) and coherency (bottom) spectra of the zonal components of wind stress (Fig. 7, center).

Power and coherency spectra of the zonal components of stress (Fig. 7, center) are shown in Fig. 8. More power is in the annual cycle and its harmonics than in the other frequencies, and the annual fluctuations are highly coherent, as expected. The peak in the northeast trades is lower than in the southeast trades because the wind strength in a fixed area north of the equator is influenced by both the annual variation in wind strength and the meridional shifting of the maximum winds, which combine to cause a strong semiannual signal in the region near 20°N. The power spectra (not presented) for the mean wind stress (Fig. 7, top and bottom) have a higher annual peak in the northeast trades, as suggested by the larger annual amplitude in Fig. 3. It is interesting that the power is small in both trades at 0.6 cycle per year (cpy) below which it increases, although the length of the record is too short to compute significant spectral values for the low frequencies. The coherency also rises at the lowest frequencies. There is considerable power in the northeast trades at higher frequencies which are not harmonics of 1 cpy, as can also be seen in Fig. 7. The higher frequency fluctuations are disturbances in the subtropics, and they appear in the zonal component of stress for the northeast but not the southeast trades because the area used for the northeast trades is located farther from the equator. Coherency is below the 95% significance level in the range of frequencies between 1 and 6 cpy. The peak at 2.5 cpy might be fortuitous since the 95% confidence level is not exceeded. The annual variation is the only certain relationship between fluctuations of the northeast and southeast trades that appears in the coherency spectra.

4. Summary and conclusions

1) The northeast and southeast trades are strongest during their respective winter and spring seasons.

2) The area covered by northeast trades is smaller than the area covered by southeast trades, but the northeast trades have a stronger mean wind stress and a larger annual variation both in area and mean stress.

3) The meridional profile of zonal wind stress changes considerably during the year, with large meridional displacements of the northeast trade wind maximum and formation of a distinct minimum between the trades near 10°N from July to October. The profile over the South Pacific changes significantly between the eastern and western Pacific.

4) The southeast trades covered an exceptionally large area and were stronger than normal during 1955–56, 1964, 1966–67 and 1970–71, preceding El Niño events.

5) The northeast trades change relatively little from year to year.

6) There is no apparent relationship between fluctuations of the northeast and southeast trades, except with the annual cycle.

Acknowledgments. We would like to thank Mrs. Shikiko Nakahara for her efforts in processing the huge number of wind data. This research was supported by the National Science Foundation and the Office of Naval Research under the North Pacific Experiment of the International Decade of Ocean Exploration. This support is gratefully acknowledged.

REFERENCES

Crowe, P. R., 1951a: The trade wind circulation of the world. *Inst. Brit. Geogr. Trans. Pap.*, No. 15, 39–56.

——, 1951b: The seasonal variation in the strength of the trades. *Inst. Brit. Geogr. Trans. Pap.*, No. 16, 25–47.

Dury, J. M., 1970: The Beaufort Scale of wind force. WMO Report on Marine Science Affairs, No. 3, 22 pp.

Hellerman, S., 1967: An updated estimate of the wind stress on the world ocean. *Mon. Wea. Rev.*, **95**, 607–614.

Kinsman, B., 1968: An exploration of the origin and persistence of the Beaufort wind force scale. Rep. 39, Chesapeake Bay Inst., Johns Hopkins University, 55 pp.

Krueger, A. F., and J. S. Winston, 1975: Large-scale circulation anomalies over the tropics during 1971–72. *Mon. Wea. Rev.*, **103**, 465–473.

Meyers, G., 1975: Seasonal variation of the Pacific north equatorial current relative to the wind field. *J. Phys. Oceanogr.*, **5**, 442–449.

Munk, W. H., 1950: On the wind-driven ocean circulation. *J. Meteor.*, **7**, 79–93.

Sadler, J. C., 1969: *Average Cloudiness in the Tropics from Satellite Observations.* East-West Center Press, 22 pp. 12 plates.

Sverdrup, H., 1947: Wind-driven currents in a baroclinic ocean; With application to the equatorial currents of the eastern Pacific. *Proc. Nat. Acad. Sci.*, **33**, 318–326.

Taylor, R. C., 1973: An atlas of Pacific Islands rainfall. Rep. HIG-73-9, Data Rep. No. 25, Hawaii Inst. Geophys., University of Hawaii, 175 pp.

Wentworth, C., 1949: Directional shift of trade winds at Honolulu. *Pacific Sci.*, **3**, 82–86.

Wyrtki, K., 1975: El Niño—The dynamic response of the equatorial Pacific Ocean to atmospheric forcing. *J. Phys. Oceanogr.*, **5**, 572–584.

——, and G. Meyers, 1975a: The trade wind field over the Pacific Ocean. Part I. The mean field and the mean annual variation. Rep. HIG-75-1. Hawaii Inst. Geophys., University of Hawaii, 26 pp.

——, and ——, 1975b: The trade wind field over the Pacific Ocean. Part II. Bimonthly fields of wind stress: 1950 to 1972. Rep. HIG-75-2, Hawaii Inst. Geophys., University of Hawaii, 16 pp.